# SEARCHING FOR BENCHMARK BROWN DWARF COMPANIONS TO SUBGIANT STARS.

Nuffield Report

Alex Ogden

Roundwood Park School
Nuffield Research Placement at the School of Physics, Astronomy and Mathematics at the University of Hertfordshire, mentored by Federico Marocco and Professor David Pinfield.

# CONTENTS

# ABSTRACT / EXECUTIVE SUMMARY

The aim of this project is to produce a list of benchmark systems containing a brown dwarf and a companion subgiant star by analysing a list of potential candidates.

Brown dwarfs have very complicated atmospheres compared to other objects like stars and as a result have very complicated spectra. This means much is still unknown about brown dwarfs. One way to infer the properties of a dwarf is to find a binary system containing a dwarf and a subgiant star as objects in a binary often have the same age and composition. Such a system is called a benchmark system and is very useful in finding out the properties of complex objects that would otherwise be difficult to determine from the spectra and other available data. Once these properties are known they can be used to understand the spectra and this can be used to calculate the properties of other dwarfs and hence teach us more about them.

I calculate the proper motions of a list of benchmark dwarf candidates by using data from multiple astronomical surveys and compare them to their subgiant companions and then evaluate them using a mixture of visual inspection and computer data analysis. I use this to rank each candidate based on how likely it is to be a benchmark dwarf and hence produce a list of likely benchmark systems. The best of these candidates will be observed by a telescope and confirmed if they are genuine benchmark systems, if they are then they will be used in future research in understanding brown dwarfs. This is a particularly important subject as understanding the atmospheres and characteristics of brown dwarfs are a key stepping stone to understanding more about exoplanet atmospheres, since brown dwarfs act as an intermediate class of object between small stars and large gas giants.

# INTRODUCTION

Approximately 90% of the stars with a mass over 0.5 $M_\odot$, that we have observed, are on the main sequence (Arnett, 1996): the longest part of a star's life in which it releases energy via the nuclear fusion of hydrogen into helium (Atnf.csiro.au, n.d.). It is easily identifiable on a Hertzsprung-Russel Diagram (see Fig 1.) as a dense band of stars in the centre of the graph where the luminosity and temperature are proportional e.g. the higher the temperature the brighter it is.

These main sequence stars are born inside nebulae: large interstellar clouds of gas and dust. Over time, gravity causes the gas to clump together into GMCs (giant molecular clouds) and if the nebula is dense enough, then these clumps can form stars (if this happens then the region is called a stellar nursery). Stars are born from these clouds when they undergo gravitational collapse, which can be initiated by a number of causes. One cause of gravitational collapse is the cloud's mass. The clouds attract more gas via gravity, and the more gas they have, the stronger their gravity is so the more gas they can attract: therefore, their mass is always increasing. As the mass increases, the pressure on the inside of the cloud increases and this forces



Figure 1. A Hertzsprung-Russel Diagram plotted from the Hipparcos and Gilese Catalogues (Powell, n.d.)

the molecules closer together; causing them to lose gravitational potential energy and gain kinetic energy (this collapsing cloud is a stellar embryo). The molecules lose their kinetic energy as thermal energy when they collide with each other which increases the temperature of the cloud. This energy is given off as infrared radiation. Eventually the cloud gathers enough mass to become too dense for the radiation to escape and this causes the temperature of the cloud to rise rapidly, when this happens the cloud is classified as a protostar. As the protostar continues to collapse, the temperature inside continues to rise until it is so great that nuclear fusion of deuterium begins where deuterium and a proton fuse into helium-3:

$$^2_1\text{H} + \text{p}^+ \rightarrow \, ^3_2\text{He}$$
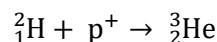
The protostar also has stellar winds which blow away any residual gas from its parent GMC and once both this and fusion has occurred then it is now a visible, pre-main sequence (PMS) star. Eventually the star collapses enough that



Figure 2. A Hertzsprung-Russel Diagram showing the Hayashi and Henyey tracks of protostars of various masses (Evolutionary Paths, n.d.)

hydrogen is fused into helium and it is now on the main sequence. Protostars can be found on the far right of H−R diagrams and they slowly move towards the central main sequence band as they age and evolve into PMS and main sequence stars (see Fig. 2). The initial downwards path of the protostar is called a Hayashi track and is caused by the size and luminosity of the star decreasing as it contracts (Hayashi, 1961). The latter horizontal path is a Henyey track and is caused by the increase in temperature when nuclear fusion begins (Henyey, Lelevier and Levée, 1955). The gravitational collapse that starts these processes can also be triggered by external events such as the shockwave from a supernova or collisions between 2 GMCs. (Atnf.csiro.au, n.d.)
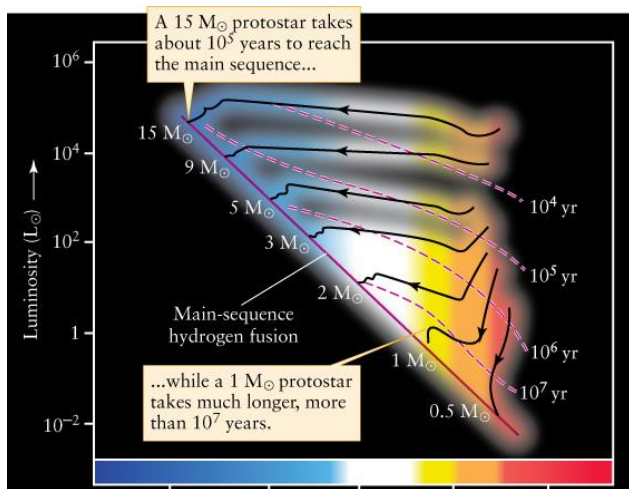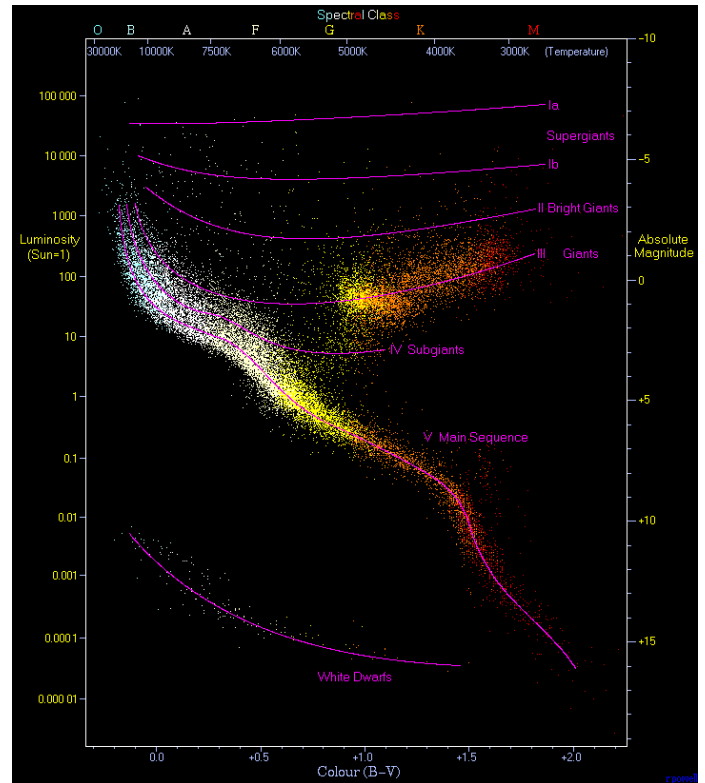
However, this only happens if the mass of the protostar is large enough to attract sufficient volumes of gas to trap the radiation inside the core to eventually start fusion. If the mass is too low,

(lower than 0.08 $M_\odot$ (Hayashi and Nakano, 1963)) then the cloud never reaches the temperatures required for hydrogen fusion and never becomes a main sequence star. Instead, electron degeneracy pressure stops the cloud from collapsing and leaves it as a substellar object between the mass of a gas giant and a star (between a debated 13-65 $M_J$). These objects are known as brown dwarfs or failed stars. There are many reasons as to why a protostar might be too small to become a star and instead becomes a brown dwarf. One mechanism is that smaller stellar nurseries get ejected from GMCs due to dynamic interactions it has with larger nurseries in a system with it. The smaller nursery will therefore have less material to gather and may then become a brown dwarf (Reipurth and Clarke, 2001). Another idea is that brown dwarfs form from the edges of protostellar discs surrounding larger main sequence stars; creating a binary system. This binary is often torn apart by passing near other stars which then causes the brown dwarf to be in its own system (Goodwin and Whitworth, 2007).

Only the youngest and heaviest brown dwarfs are hot enough to sustain some deuterium fusion, most of them simply radiate their energy as infrared radiation as they cool slowly over time, meaning that they are cold and dim compared to stars, hence why they took until 1995 to be observed (Rebolo, Osorio and Martín, 1995). Consequently, brown dwarfs are found on the bottom end of the main sequence band. Their atmospheres are very complicated as they are sometimes cool enough to allow molecules to form which means brown dwarfs need extra spectral classes to compensate for this. Some brown dwarfs are in the M class and are called late-M dwarfs, they are characterised by metal oxide absorption bands. Slightly cooler dwarfs are cool enough to have absorption bands from metal hydrides, these are called L dwarfs. T dwarfs are even cooler and they are sometimes called methane dwarfs due to large amounts of methane in their atmospheres. The coolest dwarfs are Y dwarfs and can have temperatures as low as ovens or the human body (Luhman, Burgasser and Bochanski, 2011), this is low enough to allow the formation of water and ammonia in their atmospheres (Leggett et al., 2009). Dwarfs with effective temperatures below 2,700K are known as ultracool dwarfs.

The problem is that this makes the spectra of the brown dwarfs complex and difficult to understand and, as such, there are lots of things still unknown about brown dwarfs such as the physics of their atmospheres and their initial mass function (Jeffries, 2012). It is very important to understand more about brown dwarfs because they could teach us more about gas giants since they have similar effective temperatures and structures. This is a crucial step in understanding more about extrasolar systems and exoplanets.

One way to learn more about brown dwarfs is by finding a binary system containing a brown dwarf and a star. Objects in binary systems often have very similar properties (e.g. age and chemical composition) because they are formed from the same nebula, so if the star's spectrum is observed and its properties are deduced, then it can be assumed that the brown dwarf will share these. If this is the case, then the star is known as the primary, the dwarf is known as the companion or as a benchmark dwarf and the system, as a whole, is called a benchmark system. It is quite difficult to infer the age of a star on the main sequence, however, as they do not change their appearance during this time: a star reaching the end of the main sequence is indistinguishable from the same star when it was halfway along, or when it had just entered the main sequence. The only main sequence star we know the current age of is the sun as we can use radioactive dating and helioseismology to determine its age (Bonanno, Schlattl and Paternò, 2002). It is much easier to determine the age of a



Figure 3. Artist's Impression of a T Dwarf (Hurt, 2006).

subgiant star though. Subgiant stars are stars which have finished the main sequence, as they have exhausted their hydrogen to fuse in their core, but which haven't fully evolved into a giant star yet. They are found slightly above the main sequence on the Hertzsprung-Russel Diagram. In astronomical terms, the subgiant phase is negligible (sometimes only a few million years (Salaris and Cassisi, 2005)) which means that you can approximately calculate the star's age by calculating its expected lifetime on the main sequence. This means that benchmark systems with subgiant stars are particularly useful.

For a star and a brown dwarf to be in a binary, they must be in the same area of sky and have a common proper motion. Proper motion (μ) is the angular velocity of a star compared to the background stars, as seen from the sun (Koupelis and Kuhn, 2007). It is calculated twice; once each for the Right Ascension (RA or α) and once for Declination (DEC, DE or δ). RA and DEC are the co-ordinates used to describe the positions of objects in the sky, analogous to Longitude and Latitude on the ground (see Fig. 4). They can be measured in either degrees or in sexagesimal, in this project they will be recorded in degrees. Proper motion is calculated as the change in RA or DEC over time (t):



$$\mu_\alpha = \frac{d\alpha}{dt} \qquad \mu_\delta = \frac{d\delta}{dt}$$

These 2 values are the two components of total proper motion:

*Figure 4. Diagram of RA and DEC of a star as seen outside the celestial sphere (RA and DEC on celestial sphere.png, 2012).*

$$\mu = \sqrt{\mu_\alpha^2 + \mu_\delta^2}$$

Thus, proper motion is measured in a unit of angle size over a unit of time, usually it is milliarcseconds per year (mas/yr). The separate components of proper motion are useful for comparing the direction that the stars are traveling in whereas the total proper motion is useful for comparing the magnitudes. To calculate the change in RA and DEC for an object over time you need to take multiple measurements of RA and DEC at certain times or epochs.

This is only true due to Kepler's 3$^{rd}$ Law which states that for an object in orbit, the period (T) is proportional to the semi-major axis of the ellipse (a) (Osserman, 2001):

$$T^2 \propto a^3$$

In other words, the further away the object is, the longer it will take to complete an orbit. Brown dwarfs often orbit at a great distance from their primary star which means they have a very long orbital period. This means that it takes hundreds or thousands of years for the dwarf's orbit around the star to influence its proper motion, so that when we measure the proper motion it is unaffected by the orbit. However, if the object orbits at a smaller distance from the star, then it will orbit around the star between epochs and this will affect the proper motion calculation.

During my project, I used data from the following astronomical surveys:

o **2MASS** – Two Micron All Sky Survey is a near-infrared survey which operated from 1997-2001 and imaged the entire sky. It operated in 3 wavelength bands: J (1.235 μm), H (1.662 μm) and K$_s$ (2.159 μm) (Irsa.ipac.caltech.edu, n.d.) (see glossary entry: Photometric Bands).
o **SDSS** – Sloan Digital Sky Survey is an optical survey that has imaged a 3$^{rd}$ of the sky in the g, r, i, z and y bands (Sdss.org, 2017).
o **WISE** – Wide-field Infrared Survey Explorer is a mid-infrared survey with its own bands: W1 (3.4 μm), W2 (4.6 μm), W3 (12 μm) and W4 (22 μm). It has imaged the entire sky. It operated in 2009 and 2010 (Irsa.ipac.caltech.edu, 2017).
o **ULAS** – UKIDDS Large Area Survey is an infrared survey in bands Y, J, H and K which covered 4000 sq degrees of sky (Ukidss.org, n.d.).
o **PanSTARRS** – Panoramic Survey Telescope and Rapid Response System is an ongoing optical survey that images in g, r, i, z and y bands (Panstarrs.stsci.edu, n.d.).
o **UHS** – UKIRT Hemisphere Survey is a 12,700 sq degrees survey in the J band to cover a large portion of the northern hemisphere along with the UKIDDS surveys. It is currently unavailable to the public and is only available to certain scientists (Dye et al., 2017).
o **TGAS** – Tycho-Gaia Astrometric Solution is a combination of the surveys Gaia and Tycho-2 which has calculated the proper motions of 2.5 million stars (Michalik, Lindegren and Hobbs, 2015).
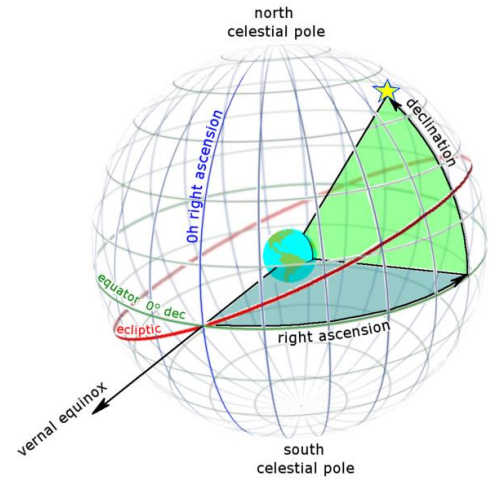
## PROJECT AIMS

The aim of my project is to evaluate a list of candidate brown dwarfs for their potential to be companions with primary sub-giant stars and therefore produce a collection of potential benchmark systems.

## METHOD

The first step was to generate a list of brown dwarfs which were close enough to a subgiant star to be in a binary. This was provided by my mentor. These dwarfs were found by a code which searched for brown dwarf like objects in a 3-arcminute radius around known subgiant stars, ignoring the galactic plane as this is too bright and densely packed to precisely detect the dwarfs. However, brown dwarfs look very similar to many other dim red objects in the sky for example: galaxies and quasars. This meant that each candidate found by the code needed to be visually inspected to remove any candidates that were clearly not brown dwarfs. There were 2 lists of candidates that this needed to be done for; optical detections and optical non-detections. The optical detections contained candidates which were visible in the optical spectrum, 73 detected by UHS and 4 detected by ULAS. The optical non-detections were those candidates that were visible in the infrared but they weren't detected by SDSS-DR9, this was comprised of 108 candidates all from ULAS. During my visual inspection, I used the following criteria:
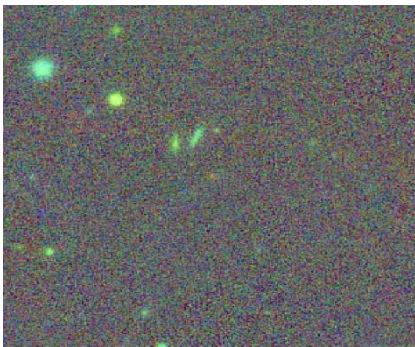


*Figure 5. PanSTARRS Image of a faint red point source (TYC 4-1167-1, Random Index of 1137794) near 2 extended source galaxies (PanSTARRS, 2016).*

Firstly, the object must be a point source and not an extended source. A point source is a source of light that is circular and well defined, as opposed to being an oval shape like an extended source. The reason for this is that brown dwarfs are small spherical objects and so should look like faint point sources and galaxies are usually extended sources. This criterion should therefore cut out any galaxies from the candidate list.

The object must also be very faint in the optical spectrum and brighter in the infrared spectrum i.e. is bright in the y band but gets gradually less visible going up to the g band. This is because brown dwarfs are very cool and so emit light with a lower energy than other objects i.e. they will emit infrared more strongly than they emit visible light, if they emit any visible light at all.
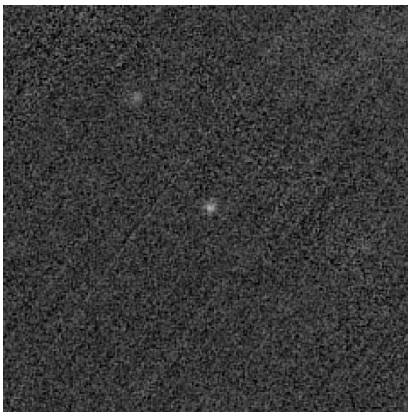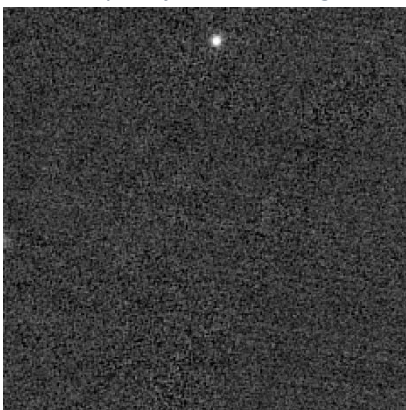

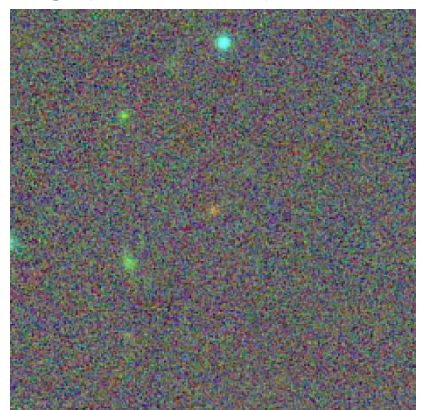
G band
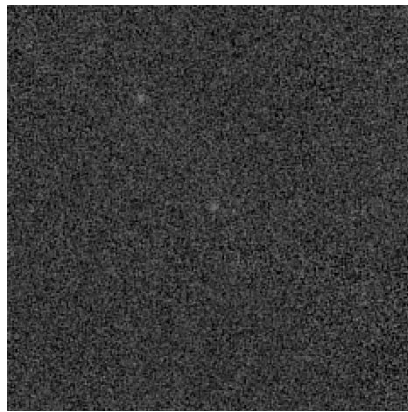


Y band
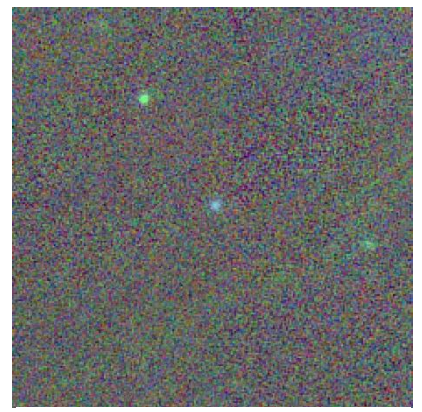


False Colour

*Figure 6. HIP 6303 (Random Index 1165800) is clearly visible in g band and less visible in y band, this means it is unlikely to be a brown dwarf. Additionally, the false colour image shows this object as blue whereas most of the dwarfs were red or orange. (PanSTARRS, 2016)*



G band



Y band



False Colour

*Figure 7. TYC 60-858-1 (Random Index 1959516) is invisible in the g band but visible in the y band, this means it is likely to be a brown dwarf. It also appears red in the false colour image and this is expected for a brown dwarf. (PanSTARRS, 2016)*

Sometimes an object would already be identified and categorised by another survey. Clearly, if an object was identified as something other than a brown dwarf then it would be removed. This was useful for objects such as faint quasars and galaxies which could otherwise be confused for a brown dwarf.

Diffraction spikes can also be a problem as they can be mistaken for stars by the telescope or can obscure other stars. Most diffraction spikes are edited out of the images uploaded by the surveys but they can still cause problems. If an object appeared to be an error due to a diffraction spike then it was removed.

Incredibly bright stars also caused some issues during visual inspection as they can saturate the image. This is where a star is so bright that the brown dwarf cannot be seen because the brightness resolution that the pixels can display is too small. The solution to this is to zoom in on the image so that the dwarf can be seen (see Figure 11).



*Figure 8. TYC 254-576-1 (Random Index 1245886) was identified as a quasar as it looks pink in the false colour image and appears in some quasar surveys e.g. HMQ Catalogue. (PanSTARRS, 2016)*

This process removed 47 candidates from the optical detections (leaving 30 remaining) and 11 from the optical non-detections (leaving 97 remaining). The reason that so many were removed from the optical detections was because of the Andromeda Galaxy. Andromeda has a similar effect to the galactic plane in that it's so densely packed that it is very difficult to detect the movement of stars with any precision. Unfortunately, one of the subgiant companions that was searched around (Source ID: 3.69247E+17) was in front of andromeda which meant that 43 dim red objects in andromeda were detected as candidates. These objects were all rejected as it is unlikely that one star has 43 brown dwarf companions: even if one of them was a brown dwarf, it would be very difficult to measure its proper motion.
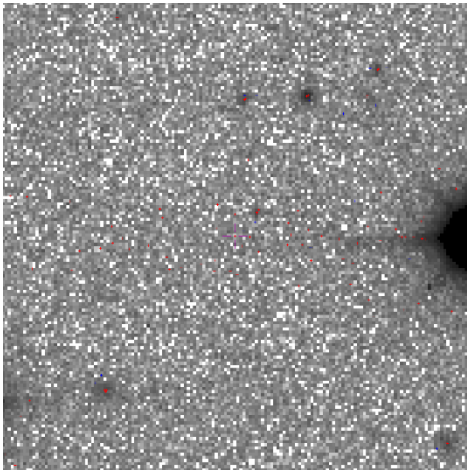


*Figure 9. Y band image of TYC 242-1337-1 (Random Index 399231, shown as purple cross) in Aladin shows it is likely to be a diffraction spike as it is not in the image but it is part of a long line of detections (red crosses) that could be a removed diffraction spike. (ULAS, 2008)*
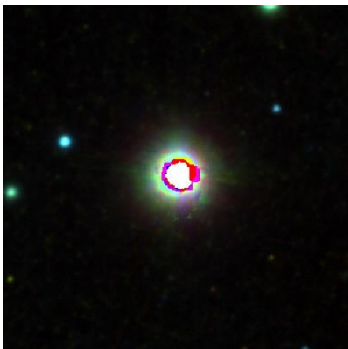


*Figure 10.
(Left) the subgiant star in proximity to Andromeda. (PanSTARRS, 2016)
(Right) An example of the difficulty of identifying and tracking stars in Andromeda. (PanSTARRS, 2016)*
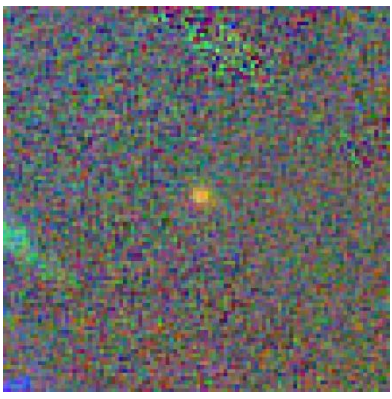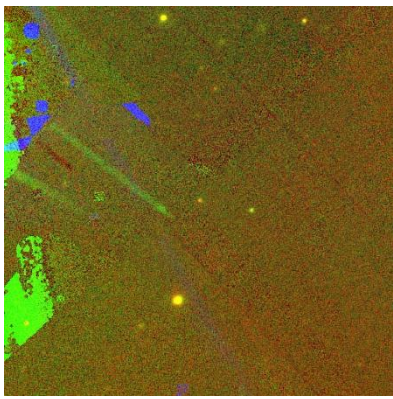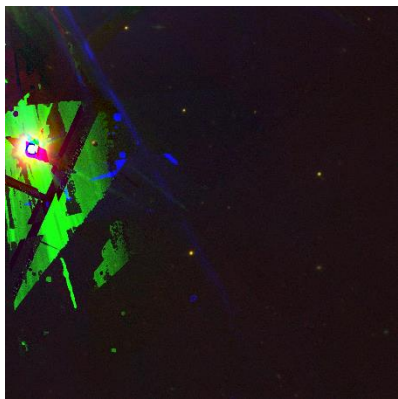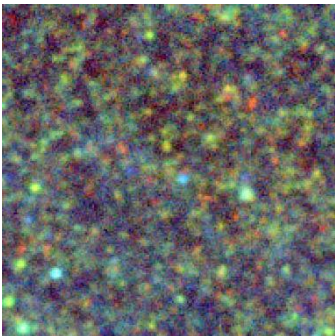


*Figure 11. Successive zooming into TYC 870-99-1 (Random Index 1439409) reduces the image distortion from a very bright star (β Leo, the 2ⁿᵈ brightest star in the Leo constellation) (PanSTARRS, 2016)*

Once the objects had been visually inspected, the next step was to collect more epochs so that the proper motion could be calculated. I used VizieR and Aladin to do this. VizieR is a database that returns a list of all the astronomical surveys contain an object within a certain radius of co-ordinates you supply. Aladin is an astronomical image editing software that allows you to compare and edit images of the sky.

Once the image is uploaded to Aladin it may need to undergo some pixel mapping edits so that the objects can be seen. After this I compared images from ULAS and PanSTARRS and opened lots of surveys in Aladin so that I could confirm that the VizieR results were actually the dwarf and not another nearby object or non-detection.
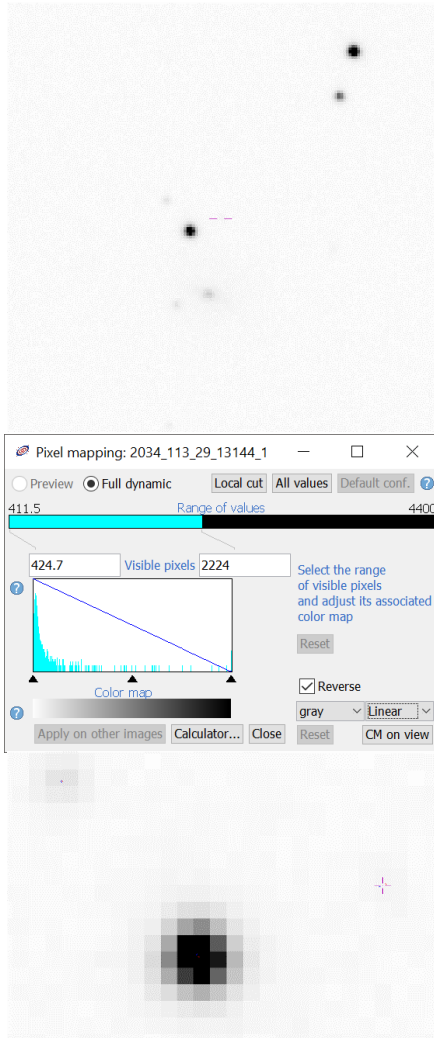


*Figure 12. (ULAS, 2009)*

*In the original FITS File (left) from ULAS, the dwarf at the purple cross cannot be seen.*

*When it is edited using the pixel mapping tool on Aladin it becomes visible (right). This means that it is possible to check whether the VizieR database search results have identified the correct object or whether it is in fact a nearby different object, this can obviously only be determined when all the objects are visible in the image. The images at the bottom illustrate this, the red and blue point represent VizieR results for a survey that identified that object. In the edited image, it is easy to see which object each point corresponds to. In the non-edited image, however, it is impossible to know whether the points correspond to an object or are just errors in the survey's data.*

*The cyan histogram shows how many pixels are at each colour value on the colour map below. The background noise is the steep curve at the white end of the graph and the objects are the small fluctuations towards the black end. The dark blue line shows which pixel values are included in the image, in the edited image it starts after the peak of noise so there is no noise. It also has the form Asinh as opposed to linear which means it curves down and includes all the fainter objects at the bottom of the graph.*
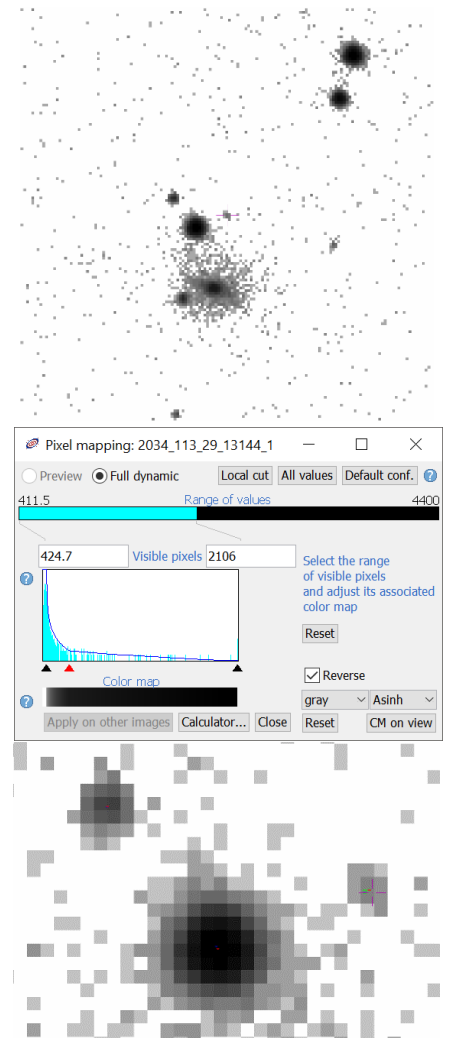
The date reference system I chose to use was MJD (Modified Julian Date) which counts the number of days since November 17th, 1858. This means that all the epochs for my candidates were in the MJD format. However, some surveys used decimal year (like the standard calendar except that the progress through the year is recorded as a decimal rather than as months e.g. 2010.5589). To convert between these 2 systems, I used TOPCAT: an astronomical spreadsheet and data handling program. This was done using the 'decYearToMjd()' function.

After this had been done for all the candidates and recorded in a table, I converted it to a FITS file using TOPCAT so that it could be used to calculate the proper motions of the candidates. One issue was that the data in my table was recorded as a string (list of characters) but needed to be a double (64-bit number) so that it could be calculated with; this was done with the 'parseDouble(str)' function which converts the strings to doubles. All data has an uncertainty in its value due to our instruments not being 100% precise. However, some of the UKIDDS data did not have any uncertainties given for their RA and DEC values which meant that they had to be estimated using code written by Matt Rickard: one of the University's master's degree students. The code takes an existing data set of astronomical co-ordinates that has uncertainties and uses interpolation to estimate the uncertainty that another data set would have. This produces a good estimate for the uncertainty, providing that the 2 data sets are similar. In this case the data sets were similar and so the estimated errors were good enough to be used in out calculations.

My mentor Federico then used another code to automatically calculate the proper motion and uncertainties for all the candidates that passed visual inspection. I could then compare these with the proper motions of the subgiant stars calculated by TGAS and determine whether they had common proper motion. It was highly unlikely that any of the proper motion values would have been exactly the same due to the uncertainties in the values, so instead I checked whether the confidence intervals overlapped. In other words, check whether it was possible for the proper motions of both objects to be the same when considering the uncertainties. However, the TGAS calculations have negligible uncertainties and so I just checked whether the calculated value from TGAS was within the confidence interval of the brown dwarf.
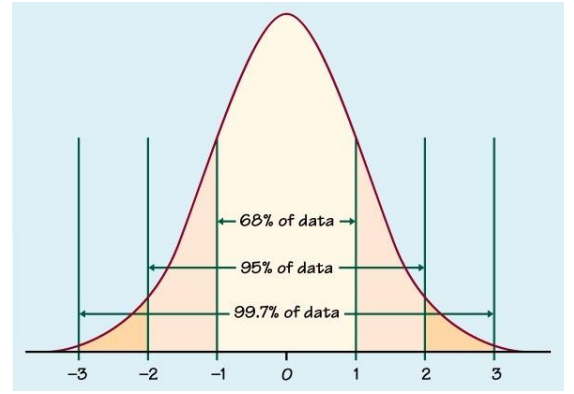


*Figure 13. It is reasonable to assume that the true value of the proper motion of the dwarf is distributed normally around the calculated value, where the standard deviation $\sigma$ is the uncertainty and the mean $\mu$ is the calculated value. Using a confidence interval of $3\sigma$ to check whether the proper motions are common is good because there is a 99.7% chance that the true value of proper motion lies within $3\sigma$ of the calculated value. Anything greater than $3\sigma$ would be too big and might show that there is common proper motion even when there isn't because any data outside $3\sigma$ is an outlier.*

I did this using the following calculation in LibreOffice Calc (equivalent to Microsoft Excel) which calculates how many multiples of the uncertainty σ the two proper motions are from each other:

$$\mu_{RA}\sigma\text{Difference} = \left| \frac{\mu_{RA_{Dwarf}} - \mu_{RA_{Subgiant}}}{\sigma_{dwarf}} \right|$$



*Figure 14. A section of my Table that checks whether the $\mu$ are less than $3\sigma$ apart. I also checked $2\sigma$ and $1\sigma$ as the lower the $\sigma$ difference is the better and an object separated by $1\sigma$ is better than one separated by $3\sigma$.*

Although μ means both proper motion and the mean, in this case it can mean both. In LibreOffice the equation looks like '=ABS((C2-I2)/D2)'. This calculation is then repeated for $\mu_{DEC}$ and if both these values are below 3 then the confidence intervals overlap. I used the following function to do this:' =IF(AND(L2<=3,M2<=3),"Yes","No")' which will print 'Yes' if the σ difference for $\mu_{RA}$ and $\mu_{DEC}$ are both less than 3 and will print no otherwise. I then ranked each object based on their σ difference using the RANK function where rank 1 would have the closest μ. An alternative method would be to calculate $\mu_{total}$ and calculate the σ difference of that instead.

An important thing to consider is the length of time the object has been measured over and the number of epochs it has. Obviously, an object with only 2 data points separated by a few months is much less accurate than an object with multiple data points over a few years as it has had more time to noticeably move. To account for this I added further criteria that the object must have at least 3 data points collected over at least 1 year using the functions '=IF(G2>=1,"Yes","No")' and '=IF(F2>=3,"Yes","No")'. I then ranked each of these criteria where rank 1 was the longest period of time and the most data points respectively.

Candidates with high uncertainties caused issues because there is such a large range of proper motions that they could take that it was highly unlikely that their true value actually overlapped with the TGAS star value. I accounted for this in 2 ways: I calculated the sum of the errors for each candidate and ranked them accordingly and I calculated the significance of the μ errors. The significance was calculated by dividing the μ by $\mu_{err}$ for both RA and DEC, therefore objects with a high significance are objects that have a low uncertainty compared to their proper motion and so objects with large uncertainties are ruled out. Each candidate was ranked for significance also where rank one had the largest significance. I also ranked each candidate on the total μ of its subgiant star, this is because most objects in the sky have a very low proper motion and so objects that have a high common proper motion are even more likely to be companions than if they had a common low proper motion.

The reliability of the data was not the only thing to consider when evaluating candidates, I also needed to consider how interesting and useful the candidate would be if it was a benchmark system. For example, objects with particularly high or low metallicities are interesting as their spectra will look different from the majority of objects with more normal

metallicities. Metallicity is measured in Fe/H which is the ratio of iron to hydrogen content in a star compared with

the sun, it is given by the following formula (Icc.dur.ac.uk, n.d.) (Note: in astronomy a metal can be taken to mean any element other than H or He, so metallicity can also be defined as the proportion of non H or He elements in a star, this is not the case in this report).

$$[Fe/H] = \log_{10}(\frac{N_{Fe}}{N_H})_{star} - \log_{10}(\frac{N_{Fe}}{N_H})_{sun}$$

The metallicity data was from TGAS and I ranked each object (with a σ difference of less than 3) based on the absolute value of its Fe/H where an object with a very different metallicity from the sun (very high or very low) would be ranked 1st and an object that was very similar to the sun (Fe/H close to 0) would be ranked last. I did this with the following function '=RANK(ABS(AK2),AK2:AK31,0)' and I also checked whether the metallicity was greater in magnitude than 0.1 with '=IF(ABS(AJ2)>=0.1,"Yes","No")'

I also needed to check whether the stars were observable on the dates when the university had access to the Cerro Tololo Observatory in Chile as the next step for my supervisors would be to take my data and use it to decide which candidates to observe with the telescope; I did this with STARALT, a program that shows when and by how much an object will be visible at a given location (Sorensen, Azzaro and Mendez, 2002). I ranked each candidate, that had a less than 3σ separation from its companion, based on the amount of time that it spent being over 30˚ above the horizon at the observatory, this is because most telescopes can't observe objects when they are too close to the horizon as this would require the telescope to decline too much (Fariña, 2015). I also ranked each candidate based on the total number of yeses.



*Figure 15. An example of the data from STARALT that shows the path of PSO J010440.567+274602.467 across the sky on 8/9/17.*

The final step to produce the overall list of which candidates were best to observe was made by taking an average of every previously made ranking and then ranking each candidate based on that. This produced a good guide to which candidates should be observed as the candidates which consistently had desirable properties (e.g. had low uncertainties and had enough epochs) would be ranked nearer 1st and candidates which consistently had undesirable properties were nearer last. In addition, I also colour coded each candidate because, although they had gone through the checks, some still had some issues. For example, some candidates may have had a proper motion that was close to their subgiant companion's but they may not have had enough epochs taken. These candidates were left in because it is still possible that they are companions but there isn't enough data currently available to determine this very accurately. A green colour code meant that there were no issues with the candidate. Yellow meant that the errors were slightly high but was otherwise okay. Orange indicated that the candidate had an issue with one of its properties e.g. high errors, low no. of epochs or small amount of time between epochs. Red indicated that there was an issue with more than one of the properties.

## RESULTS

The final lists of optically detected candidates for observation appear in the following table in rank order. Observable rank is the rank of only the candidates visible on the days of observation, the colours represent the colour code of that candidates as previously described.

| Name | Rank | Observable Rank |
|---|---|---|
| PSO J032621.964+043814.299 | 1 | 1 |
| PSO J032621.688+040110.198 | 2 | 2 |
| PSO J153915.399+411239.099 | 3 | |
| PSO J040219.288+180221.785 | 4 | 3 |
| PSO J220119.252+280030.271 | 5 | 4 |
| PSO J010440.567+274602.467 | 6 | 5 |
| PSO J034540.796+174555.478 | 7 | 6 |
| PSO J023024.087+243240.469 | 8 | 7 |
| PSO J030557.883+120253.905 | 9 | 8 |
| PSO J004309.606+452707.354 | 10 | |
| PSO J030156.314+564211.656 | 11 | |
| PSO J072000.412+050416.712 | 12 | 9 |
| PSO J030151.114+571826.053 | 13 | |
| PSO J171854.234+002459.802 | 14 | |
| PSO J030158.061+572111.509 | 15 | |

This is the same list but for the optically non-detected candidates.

| RANDOM_INDEX | RANK | OBSERVABLE_RANK |
|---|---|---|
| 1352766 | 1 | 1 |
| 705235 | 2 | 2 |
| 1174283 | 3 | |
| 853120 | 4 | 3 |
| 1521053 | 5 | 4 |
| 484684 | 6 | 5 |
| 744563 | 7 | |
| 1959516 | 8 | 6 |
| 1124392 | 9 | 7 |
| 2002595 | 10 | 8 |
| 806947 | 11 | |
| 622549 | 12 | 9 |
| 1187843 | 13 | 10 |
| 1337676 | 14 | |
| 1101440 | 15 | 11 |
| 850910 | 16 | 12 |
| 2037999 | 17 | 13 |
| 452690 | 18 | 14 |
| 622549 | 19 | 15 |
| 1101440 | 20 | 16 |
| 1811863 | 21 | 17 |
| 613371 | 22 | 18 |
| 1073604 | 23 | 19 |
| 850910 | 24 | 20 |
| 20041 | 25 | 21 |
| 1321043 | 26 | 22 |
| 248942 | 27 | 23 |
| 808045 | 28 | 24 |
| 340973 | 29 | 25 |
| 1101440 | 30 | 26 |
| 194626 | 31 | 27 |
| 1137794 | 32 | 28 |
| 395386 | 33 | 29 |
| 1268680 | 34 | 30 |
| 1526 | 34 | 30 |
| 548912 | 36 | 32 |
| 759413 | 37 | 33 |
| 1162863 | 38 | 34 |
| 1992106 | 39 | 35 |
| 1521053 | 40 | 36 |
| 1457975 | 41 | 37 |
| 639776 | 42 | 38 |
| 1281216 | 42 | |
| 689903 | 42 | 38 |
| 1870874 | 45 | |
| 634219 | 46 | 40 |
| 1199670 | 47 | |
| 1122793 | 48 | 41 |
| 1935802 | 49 | 42 |

# CONCLUSION AND EVALUATION

In conclusion, my project has successfully evaluated a list of potential brown dwarf benchmark system candidates and produced 2 ranked lists of how likely the candidates are to be benchmark systems relative to each other. The optical detections had a total of 15 potential systems whereas the non-detections yielded 49. ~19% of optical detections and ~45% of the non-detections became potential systems. The 10 most promising of these, which should be prioritised for observation, are:

| Name | Rank | Observable Rank |
|---|---:|---:|
| PSO J032621.964+043814.299 | 1 | 1 |
| 1352766 | 1 | 1 |
| 705235 | 2 | 2 |
| 853120 | 4 | 3 |
| 1521053 | 5 | 4 |
| 484684 | 6 | 5 |
| 1124392 | 9 | 7 |
| 2002595 | 10 | 8 |
| 622549 | 12 | 9 |
| 1187843 | 13 | 10 |

Of these 10 most promising systems, 1 was from the detections and 9 are from the non-detections. This means that ~1% of the total optically detected and ~8% of the non-detected candidates were in this promising set. The large number of candidates in front of/in andromeda in the optical detections is the reason that there are fewer potential systems from the detections compared with the non-detections.

I think my project will yield good results as my methods were approved by my mentors and were similar to methods that they themselves had used in the past for similar work. Additionally, as my data set was relatively small it meant that I could visually inspect all my candidates thoroughly and I was very involved during the entire process. This allowed me to check for errors and manually check some of the automated operations made by the computer which meant that my results' reliabilities are improved.

To check whether my colour coding system was reliable I plotted a graph of the colour code against the overall rank which I calculated. The Pearson product-moment correlation coefficient was calculated for the candidates in both data sets and there was a strong positive correlation in both of ~0.81 and ~0.70. This suggests that my results are consistent with eachother as the ranking and colour coding systems both identify the same candidates as being promising.
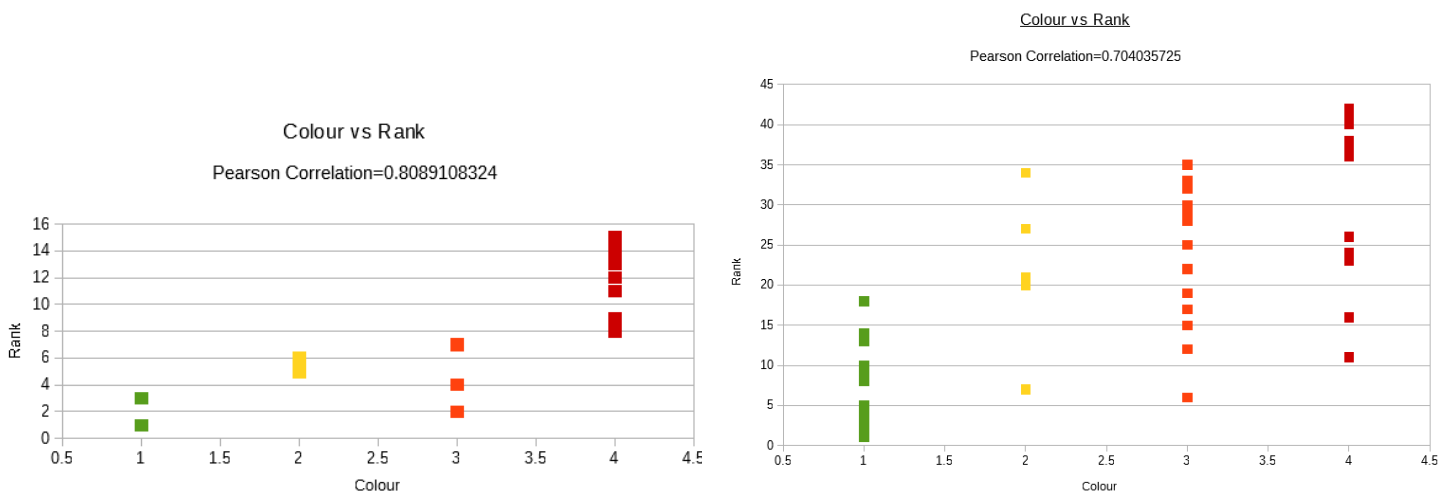


*Figure 16. Colour Code vs Rank of each candidate for optical detections (left) and non-detections (right).*

I also plotted a graph of the σ rank against the error rank. This was because the candidates I wanted were those which came near 1st in both ranks. Many candidates would have high error ranks which would lead to low sigma ranks. As expected, there is a weak negative correlation but there are some outliers with high or low values for both ranks, the most promising candidates were those which had low values for both ranks in the bottom left corners of the graphs.
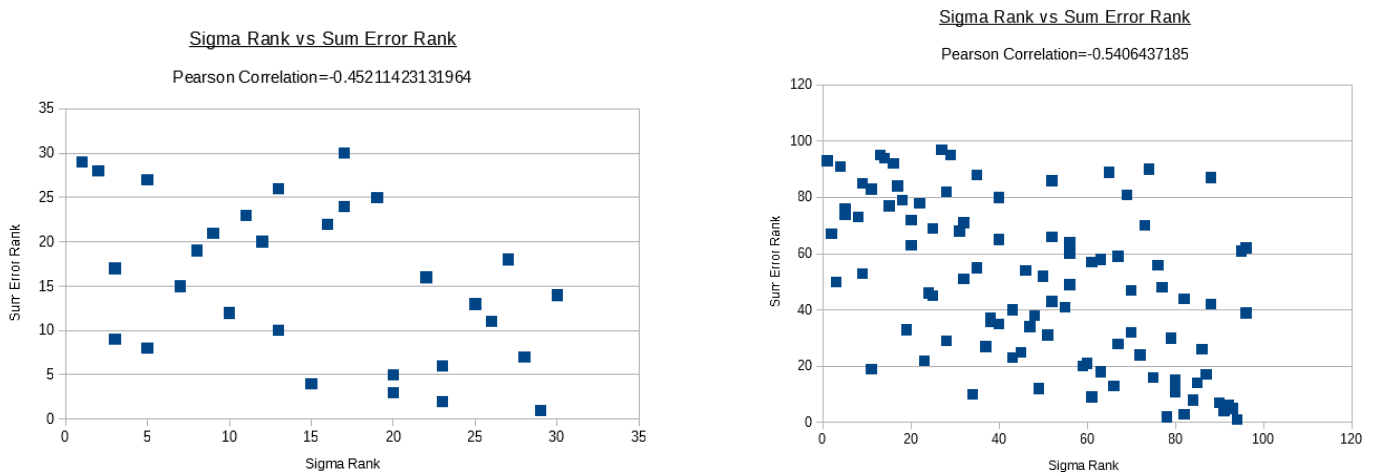


*Figure 18. Sigma Rank vs Error Rank for detections (left) and non-detections (right).*

The candidates needed to have a high significance value but also have a low sigma difference. I plotted a graph to check this. There is a positive correlation between these values and the best candidates (lighter blue) will sit slightly above the others, roughly below 2σ and above a significance of 2.
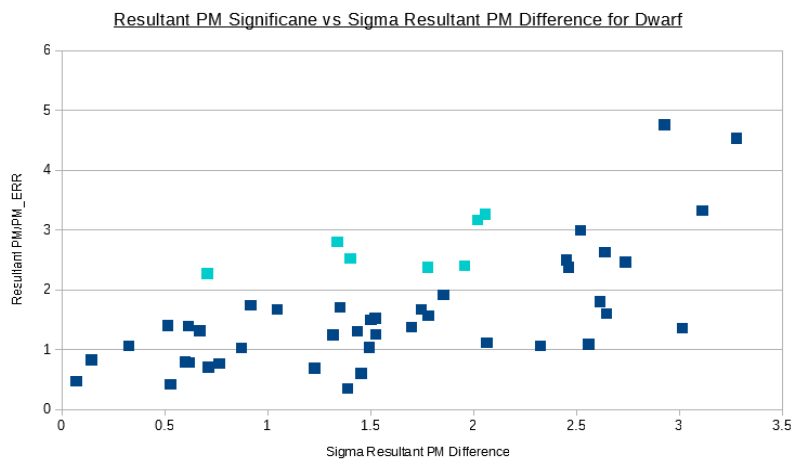


*Figure 19. Resultant PM Significance vs Resultant Sigma Difference for non-detections, best candidates have been coloured blue.*

A weakness of my project is that it is introspective. The candidates have been successfully evaluated against each other and those in the final list are definitely the most likely to be benchmark systems. However, I did not compare them to any already known benchmark systems and so if I were to repeat the project I would have compared my candidates to other previously studied candidates to check that my conclusions were consistent. One candidate (random index 689903) appeared in a list of known T Dwarfs (Burningham et al., 2013), this was encouraging and would have been very helpful if more candidates appeared in lists like this.

Another improvement would be to exclude andromeda from the code that searched for the candidates as it was initially rather puzzling as to why the sky was so busy in half of the detection candidates and not the second half. I also think that I should have been more consistent with the naming of the candidates as for the optical detections I used the PanSTARRS name but for the non-detections I used the Random Index from TGAS as not all of the candidates were identified in PanSTARRS. This was not a major issue but the process would have been much easier with more consistent and transferrable naming systems throughout the project.

One unfortunate issue was that the spectrometer at the telescope broke during the course of my project and meant that my candidates' spectra couldn't be observed and compared with their subgiant companions' spectra. However, some candidates could still be observed if they needed a better value of proper motion to be calculated e.g. if they had high errors or not enough epochs. I created another set of lists for these candidates needing more epochs to be observed on the night that the spectrometer was broken for the optical detections (top) and non-detections (bottom).

| Name | Observing Order |
| --- | --- |
| PSO J010440.567+274602.467 | 1 |
| PSO J023024.087+243240.469 | 2 |
| PSO J030557.883+120253.905 | 3 |
| PSO J072000.412+050416.712 | 4 |

| Random Index | Observing Order |
| --- | --- |
| 1124392 | 1 |
| 1101440 | 2 |
| 1073604 | 3 |
| 20041 | 4 |
| 1321043 | 5 |
| 248942 | 6 |
| 808045 | 7 |
| 340973 | 8 |
| 1101440 | 9 |
| 1137794 | 10 |
| 1162863 | 11 |
| 1457975 | 12 |
| 639776 | 13 |
| 634219 | 14 |

In order to be observed to a suitable degree of accuracy in a short space of time, the object needed to have a relatively high proper motion of over 50 mas/year. I then selected those objects which had either high errors or not enough epochs and ranked them based on their average overall rank and their colour code e.g. a candidate that has slightly too high errors that has been colour coded as yellow is much more likely to be a benchmark system (and worthwhile to observe) than one with a red colour code that has much higher errors.

## FUTURE WORK

If my candidates are confirmed to be benchmark systems then they will be used in future research to learn more about the properties of brown dwarfs. Their spectra will be measured and will have their proper motions measured more accurately with observatory telescopes to completely confirm the companionship between the subgiant and the dwarf. The subgiants will have their composition and age calculated which will then be shared by the brown dwarf, thus enabling the properties of the brown dwarf to be inferred. This will hopefully reveal many interesting properties held by the dwarf such as its metallicity, which can then be compared to its spectra to help understand some of its features.

## GLOSSARY

- **Arcminute** – 1/60 of a degree
- **Arcsecond** – 1/60 of an arcminute, 1/3600 of a degree
- **Astronomical survey** – A set of images of the sky which don't focus on one individual object
- **Benchmark Dwarf** – a brown dwarf in a benchmark system whose properties have been inferred from its primary star.
- **Benchmark System** – a system containing a star and a companion brown dwarf.
- **Binary System** – a system containing 2 stars.
- **Brown Dwarf** – (also known as a failed star) a substellar object formed in the same way as stars but which doesn't fuse hydrogen. They have masses between the smallest stars and the heaviest gas giant planets (~13-65 $M_J$)
- **Effective Temperature** – the temperature of an object calculated from the radiation it emits, assuming it is a black body.
- **Epoch** - an arbitrarily fixed instant of time or date, usually the beginning of a century or half century, used as a reference in giving the elements of a planetary orbit or the like (Dictionary.com, n.d.).
- **Exoplanet** – a planet around a star that isn't the sun.
- **Extrasolar System** – a system of stars and planets outside of the solar system.
- **FITS** – Flexible Image Transport System, a file format used for scientific data. It can be an image with information about that image's position in the sky or can be a table of data
- **Helioseismology** – studying waves on the surface of the sun to understand more about its internal structure
- **Hertzsprung-Russel Diagram** – A graph that plots the luminosity/absolute magnitude of a star on the y-axis against the colour/spectral class/temperature on the x-axis. Stars only appear in certain regions of the diagram and the different regions on the graph correspond to the different types of stars (shown by the purple writing in Fig. 1).
- **HMQ** – Half Million Quasars Survey
- $M_\odot$ - Mass of the sun, this is used to compare the masses of other stars to the sun e.g. if a star is 3 times as massive as the sun then it is said to have a mass of 3 $M_\odot$.
- $M_J$ – Mass of Jupiter, this is used to compare masses of astronomical objects with Jupiter.
- **MJD –** Modified Julian Date, an epoch that counts from 17/11/1858.
- **Milliarcsecond** – 1/1000 of an arcsecond, 1/3600000 of a degree
- **Nebula** – An interstellar cloud of gas and dust, dense collections of hydrogen gas can cause the birth of stars in stellar nurseries inside some nebulae.
- **Photometric Bands** – a method of dividing up the electromagnetic spectrum into sections. One common photometric system is to use letters, in the project the bands used are: G, R, I, Z, Y, J, H, K. which ranges from the middle of the optical to the near-Infrared. These letters are not standards and some surveys have slight variations but they are all similar. Some of the letters relate to their position on the spectrum e.g. G means green, R means Red and I means Infrared.
- **PMS Star** – A pre-main sequence star is a star that is no longer a protostar but has not yet reached the main sequence.
- **Primary Star** – the normal star in a benchmark system that the brown dwarf orbits.
- Proper Motion – the angular velocity of a star compared to the background stars, as seen from the sun (Koupelis and Kuhn, 2007)
- **Protosta**r – stage in a star's life after the collapse of the gas cloud but before it begins nuclear reactions at its core.
- **Stellar Embryo** – a GMC that has begun to collapse and will eventually become a protostar.
- **Stellar Nursery** – a region within a dense nebula in which gas and dust are contracting, resulting in the formation of new stars (En.wiktionary.org, 2016).
- **Subgiant Star** – stars which have finished the main sequence, as they have exhausted their hydrogen to fuse in their core, but which haven't fully evolved into a giant star yet.
- **TGAS** – Tycho-Gaia Astrometric Solution.
- **UKIDDS** – UKIRT Infrared Deep Sky Survey.
- **UKIRT** – United Kingdom Infrared Telescope.

# REFERENCES (in order of appearance)

- Arnett, D. (1996). *Supernovae and nucleosynthesis*. Princeton, N.J.: Princeton Univ. Press.
- Atnf.csiro.au. (n.d.). *Main Sequence Stars Australia Telescope National Facility*. [online] Available at: http://www.atnf.csiro.au/outreach//education/senior/astrophysics/stellarevolution_mainsequence.html [Accessed 29 Aug. 2017].
- Powell, R. (n.d.). *HRDiagram*. [image] Available at: https://upload.wikimedia.org/wikipedia/commons/6/6b/HRDiagram.png [Accessed 29 Aug. 2017].
- Evolutionary Paths. (n.d.). [image] Available at: http://www.public.asu.edu/~atpcs/atpcs/Univ10e/Images/6592_fig18_10.jpg [Accessed 29 Aug. 2017].
- Hayashi, C. (1961). Stellar evolution in early phases of gravitational contraction. *Astronomical Society of Japan*, [online] 13, pp.450-452. Available at: http://articles.adsabs.harvard.edu/cgi-bin/nph-iarticle_query [Accessed 29 Aug. 2017].
- Henyey, L., Lelevier, R. and Levée, R. (1955). The Early Phases of Stellar Evolution. *Publications of the Astronomical Society of the Pacific*, [online] 67, p.154. Available at: http://iopscience.iop.org/article/10.1086/126791/pdf [Accessed 29 Aug. 2017].
- Atnf.csiro.au. (n.d.). *Star Formation Australia Telescope National Facility*. [online] Available at: http://www.atnf.csiro.au/outreach/education/senior/astrophysics/stellarevolution_formation.html [Accessed 29 Aug. 2017].
- Hayashi, C. and Nakano, T. (1963). Evolution of Stars of Small Masses in the Pre-Main-Sequence Stages. *Progress of Theoretical Physics*, 30(4), pp.460-474.
- Reipurth, B. and Clarke, C. (2001). The Formation of Brown Dwarfs as Ejected Stellar Embryos. *The Astronomical Journal*, 122(1), pp.432-439.
- Goodwin, S. and Whitworth, A. (2007). Brown dwarf formation by binary disruption. *Astronomy & Astrophysics*, 466(3), pp.943-948.
- Rebolo, R., Osorio, M. and Martín, E. (1995). Discovery of a brown dwarf in the Pleiades star cluster. *Nature*, 377(6545), pp.129-131.
- Luhman, K., Burgasser, A. and Bochanski, J. (2011). DISCOVERY OF A CANDIDATE FOR THE COOLEST KNOWN BROWN DWARF. *The Astrophysical Journal*, 730(1), p.L9.
- Hurt, R. (2006). *T Dwarf*. [image] Available at: https://commons.wikimedia.org/w/index.php?curid=2133578 [Accessed 31 Aug. 2017].
- Leggett, S., Cushing, M., Saumon, D., Marley, M., Roellig, T., Warren, S., Burningham, B., Jones, H., Kirkpatrick, J., Lodieu, N., Lucas, P., Mainzer, A., Martín, E., McCaughrean, M., Pinfield, D., Sloan, G., Smart, R., Tamura, M. and Van Cleve, J. (2009). THE PHYSICAL PROPERTIES OF FOUR ~600 K T DWARFS. *The Astrophysical Journal*, 695(2), pp.1517-1526.
- Jeffries, R. (2012). Measuring the Initial Mass Function of Low Mass Stars and Brown Dwarfs. *EAS Publications Series*, 57, pp.45-89.
- Salaris, M. and Cassisi, S. (2005). *Evolution of Stars and Stellar Populations*. New York, NY: John Wiley & Sons, p.142.
- Bonanno, A., Schlattl, H. and Paternò, L. (2002). The age of the Sun and the relativistic corrections in the EOS. *Astronomy & Astrophysics*, 390(3), pp.1115-1118.
- Koupelis, T. and Kuhn, K. (2007). *In quest of the universe*. Sudbury, Mass [u.a.]: Jones and Bartlett Publ, p.369.
- Ra and dec on celestial sphere.png. (2012). [image] Available at: https://commons.wikimedia.org/wiki/File:Ra_and_dec_on_celestial_sphere.png [Accessed 4 Sep. 2017].
- Osserman, R. (2001). Kepler's Laws, Newton's Laws, and the Search for New Planets. *The American Mathematical Monthly*, 108(9), p.813.
- Irsa.ipac.caltech.edu. (n.d.). *IRSA - Two Micron All Sky Survey (2MASS)*. [online] Available at: http://irsa.ipac.caltech.edu/Missions/2mass.html [Accessed 4 Sep. 2017].
- Sdss.org. (2017). Understanding the Imaging Data | SDSS. [online] Available at: http://www.sdss.org/dr14/imaging/imaging_basics/ [Accessed 8 Sep. 2017].
- Irsa.ipac.caltech.edu. (2017). IRSA - Wide-field Infrared Survey Explorer. [online] Available at: http://irsa.ipac.caltech.edu/Missions/wise.html [Accessed 8 Sep. 2017].

- Ukidss.org. (n.d.). *UKIDSS Surveys*. [online] Available at: http://www.ukidss.org/surveys/surveys.html [Accessed 10 Sep. 2017].
- Panstarrs.stsci.edu. (n.d.). *The Pan-STARRS1 data archive home page*. [online] Available at: https://panstarrs.stsci.edu/ [Accessed 10 Sep. 2017].
- Dye, S., Lawrence, A., Read, M., Fan, X., Kerr, T., Varricatt, W., Furnell, K., Edge, A., Irwin, M., Hambly, N., Lucas, P., Almaini, O., Chambers, K., Green, R., Hewett, P., Liu, M., McGreer, I., Best, W., Zhang, Z., Sutorius, E., Froebrich, D., Magnier, E., Hasinger, G., Lederer, S. and Bold, M. (2017). The UKIRT Hemisphere Survey: Definition and Full J-band Data Release. *Monthly Notices of the Royal Astronomical Society*. [online] Available at: https://arxiv.org/pdf/1707.09975v1.pdf [Accessed 10 Sep. 2017].
- Michalik, D., Lindegren, L. and Hobbs, D. (2015). TheTycho-Gaia astrometric solution. *Astronomy & Astrophysics*, 574, p.A115.
- PanSTARRS (2016). [image] Available at: http://ps1images.stsci.edu/cgi-bin/ps1cutouts?pos=2.013936+3.758576&filter=color&filter=g&filter=r&filter=i&filter=z&filter=y&filetypes=stack&auxiliary=data&size=300&output_size=1024&verbose=0&autoscale=99.500000&catlist= [Accessed 26 Sep. 2017].
- PanSTARRS (2016). [image] Available at: http://ps1images.stsci.edu/cgi-bin/ps1cutouts?pos=195.539424+28.980994&filter=color&filter=g&filter=r&filter=i&filter=z&filter=y&filetypes=stack&auxiliary=data&size=240&output_size=1024&verbose=0&autoscale=99.500000&catlist= [Accessed 26 Sep. 2017].
- PanSTARRS (2016). [image] Available at: http://ps1images.stsci.edu/cgi-bin/ps1cutouts?pos=51.590358+4.0195&filter=color&filter=g&filter=r&filter=i&filter=z&filter=y&filetypes=stack&auxiliary=data&size=240&output_size=1024&verbose=0&autoscale=99.500000&catlist= [Accessed 27 Sep. 2017].
- PanSTARRS (2016). [image] Available at: http://ps1images.stsci.edu/cgi-bin/ps1cutouts?pos=161.626528+1.471533&filter=color&filter=g&filter=r&filter=i&filter=z&filter=y&filetypes=stack&auxiliary=data&size=150&output_size=1024&verbose=0&autoscale=99.500000&catlist= [Accessed 27 Sep. 2017].
- ULAS (2008). [image] Available at: http://wsa.roe.ac.uk/cgi-bin/getImage.cgi?file=/disk21/wsa/ingest/fits/20080219_v1/w20080219_01428_st.fit&mfid=1854482&extNo=2&lx=241&hx=391&ly=1455&hy=1605&rf=180&flip=1&uniq=5745_458_32_19_2&xpos=76&ypos=75.8&band=Y&ra=146.093066&dec=6.719827 [Accessed 27 Sep. 2017].
- PanSTARRS (2016). [image] Available at: http://ps1images.stsci.edu/cgi-bin/ps1cutouts?pos=177.215315+14.498329&filter=color&filter=g&filter=r&filter=i&filter=z&filter=y&filetypes=stack&auxiliary=data&size=1000&output_size=1024&verbose=0&autoscale=99.500000&catlist= [Accessed 27 Sep. 2017].
- PanSTARRS (2016). [image] Available at: http://ps1images.stsci.edu/cgi-bin/ps1cutouts?pos=10.629998546405837+40.95352343724886&filter=color&filter=g&filter=r&filter=i&filter=z&filter=y&filetypes=stack&auxiliary=data&size=300&output_size=1024&verbose=0&autoscale=99.500000&catlist [Accessed 27 Sep. 2017].
- PanSTARRS (2016). [image] Available at: http://ps1images.stsci.edu/cgi-bin/ps1cutouts?pos=10.5907+40.99122&filter=color&filter=g&filter=r&filter=i&filter=z&filter=y&filetypes=stack&auxiliary=data&size=200&output_size=1024&verbose=0&autoscale=99.500000&catlist= [Accessed 27 Sep. 2017].
- ULAS (2009). [image] Available at: http://wsa.roe.ac.uk/cgi-bin/getImage.cgi?file=/disk29/wsa/ingest/fits/20090201_v1/w20090201_00663_st.fit&mfid=2352171&extNo=3&lx=941&hx=1091&ly=993&hy=1143&rf=90&flip=1&uniq=2034_113_29_13144_1&xpos=76.1&ypos=75.6&band=Y&ra=113.618177&dec=24.29704 [Accessed 28 Sep. 2017].
- Normal Distribution Curve. (n.d.). [image] Available at: http://howmed.net/community-medicine/normal-distribution-curve/ [Accessed 29 Sep. 2017].
- Icc.dur.ac.uk. (n.d.). *Metallicity of stars*. [online] Available at: http://icc.dur.ac.uk/~tt/Lectures/Galaxies/TeX/lec/node27.html [Accessed 7 Oct. 2017].

- Sorensen, P., Azzaro, M. and Mendez, J. (2002). STARALT. [online] Catserver.ing.iac.es. Available at: http://catserver.ing.iac.es/staralt/index.php [Accessed 9 Oct. 2017].

- Burningham, B., Cardoso, C., Smith, L., Leggett, S., Smart, R., Mann, A., Dhital, S., Lucas, P., Tinney, C., Pinfield, D., Zhang, Z., Morley, C., Saumon, D., Aller, K., Littlefair, S., Homeier, D., Lodieu, N., Deacon, N., Marley, M., van Spaandonk, L., Baker, D., Allard, F., Andrei, A., Canty, J., Clarke, J., Day-Jones, A., Dupuy, T., Fortney, J., Gomes, J., Ishii, M., Jones, H., Liu, M., Magazzú, A., Marocco, F., Murray, D., Rojas-Ayala, B. and Tamura, M. (2013). 76 T dwarfs from the UKIDSS LAS: benchmarks, kinematics and an updated space density. *Monthly Notices of the Royal Astronomical Society*, 433(1), pp.457-497.

- Dictionary.com. (n.d.). *the definition of epoch*. [online] Available at: http://www.dictionary.com/browse/epoch [Accessed 4 Sep. 2017].

- Oxford Dictionaries | English. (n.d.). *effective temperature - definition of effective temperature in English | Oxford Dictionaries*. [online] Available at: https://en.oxforddictionaries.com/definition/effective_temperature [Accessed 1 Sep. 2017]

- En.wiktionary.org. (2016). *stellar nursery - Wiktionary*. [online] Available at: https://en.wiktionary.org/wiki/stellar_nursery [Accessed 29 Aug. 2017].

# ACKNOWLEDGEMENTS

## APPENDIX

| | | | | |
|---|---|---|---|---|
| Initial optical detection candidate list | UHS data.csv | UHSxPS1_subgiants_less_cols.fits | ULAS data.csv | ULASxPS1_subgiants_less_cols.fits |
| Initial optical non-detection candidate list | ULAS_opt_non_detections.csv | ULAS_opt_non_detections.fits | | |
| Visual inspection of optically detected candidates | List of Processed Stars.odt | | | |
| Epoch collection of optical detections | List of Co-Ordinates of Candidates in Diffe | | | |
| Visual Inspection and epoch collection of optical non-detection candidates | List of Optical non-Detection Candid | | | |
| UKIDDS data with errors | ULAS_with_errors.csv | UHS_with_errors.csv | | |
| Error calculating code | UKIDSS_ERR_CALCS_SCRIPT.py | | | |
| Proper motion comparison for optical detections | Proper_Motion_Comparison.ods | | | |
| Proper motion comparison for optical non-detections | Proper_Motion_Comparison_Ond.ods | | | |